Received: 15 February 2024 | Revised: 16 May 2024 | Accepted: 20 May 2024

DOI: 10.1111/cas.16236

ORIGINAL ARTICLE

Cancer Science WILEY

ACSL4 upregulates IFI44 and IFI44L expression and promotes the proliferation and invasiveness of head and neck squamous cell carcinoma cells

Darius Rupa[1] | Hao-Wen Chuang[2] | Chung-En Hu[1] | Wen-Min Su[1] | Shiou-Rong Wu[2] | Herng-Sheng Lee[2] | Ta-Chun Yuan[1]

[1]Department of Life Science, National Dong Hwa University, Hualien, Taiwan, ROC

[2]Department of Pathology and Laboratory Medicine, Kaohsiung Veterans General Hospital, Kaohsiung, Taiwan, ROC

Correspondence
Ta-Chun Yuan, Department of Life Science, National Dong Hwa University, No. 1, Sec. 2, Da Hsueh Road, Shoufeng, Hualien 974301, Taiwan, ROC.
Email: yuan415@gms.ndhu.edu.tw

Present address
Darius Rupa, Department of Biology Education, Borneo Tarakan University, Indonesia

Funding information
Hsinchu Science Park Bureau, Ministry of Science and Technology, Taiwan, Grant/Award Number: NSC-111-2314-B-259-001 and NSC-112-2314-B-259 -001

Abstract

Reprogramming of cellular energy metabolism, including deregulated lipid metabolism, is a hallmark of head and neck squamous cell carcinoma (HNSCC). However, the underlying molecular mechanisms remain unclear. Long-chain acyl-CoA synthetase 4 (ACSL4), which catalyzes fatty acids to form fatty acyl-CoAs, is critical for synthesizing phospholipids or triglycerides. Despite the differing roles of ACSL4 in cancers, our data showed that ACSL4 was highly expressed in HNSCC tissues, positively correlating with poor survival rates in patients. Knockdown of ACSL4 in HNSCC cells led to reduced cell proliferation and invasiveness. RNA sequencing analyses identified interferon-induced protein 44 (IFI44) and interferon-induced protein 44-like (IFI44L), encoded by two interferon-stimulated genes, as potential effectors of ACSL4. Silencing IFI44 or IFI44L expression in HNSCC cells decreased cell proliferation and invasiveness. Manipulating ACSL4 expression or activity modulated the expression levels of JAK1, tyrosine kinase 2 (TYK2), signal transducer and activator of transcription 1 (STAT1), interferon α (IFNα), IFNβ, and interferon regulatory factor 1 (IRF1), which regulate IFI44 and IFI44L expression. Knockdown of IRF1 reduced the expression of JAK1, TYK2, IFNα, IFNβ, IFI44, or IFI44L and diminished cell proliferation and invasiveness. Our results suggest that ACSL4 upregulates interferon signaling, enhancing IFI44 and IFI44L expression and promoting HNSCC cell proliferation and invasiveness. Thus, ACSL4 could serve as a novel therapeutic target for HNSCC.

KEYWORDS
ACSL4, HNSCC, IFI44, IFI44L, IFNα/β, IRF1

Darius Rupa and Hao-Wen Chuang contributed equally to this work.

1 | INTRODUCTION

Lipids, composed of fatty acids (FAs), play essential roles in biomembrane formation, energy metabolism, and cellular signaling. Deregulated FA metabolism caused by aberrant expression or activation of metabolic enzymes drives FA overproduction, leading to metabolic disorders and cancer development. Long-chain acyl-CoA synthetases (ACSLs), including ACSL1, ACSL3, ACSL4, ACSL5, and ACSL6, are essential for generating 12–20 carbon-contained long-chain fatty acyl-CoAs. Among them, ACSL4 is a unique ACSL that catalyzes the incorporation of polyunsaturated FAs into phospholipids. Furthermore, ACSL4 functions as a key modulator of ferroptosis, a cell death process caused by the iron-dependent peroxidation of lipids. Accumulating evidence indicates that ACSL4 is highly expressed in multiple cancer types, including breast, ovarian, prostate, colon, and liver cancers. However, downregulation of ACSL4 expression is also observed in lung adenocarcinoma, gastric cancer, and glioma tissues. In addition, ACSL4 plays a contradictory role as a tumor promoter or suppressor depending on the cancer type.[1,2]

Interferon (IFN)-induced protein 44 (IFI44) and IFN-induced protein 44-like (IFI44L) are encoded by genes belonging to IFN-stimulated genes, which are transcriptionally activated by type I IFN, including IFNα and IFNβ.[3,4] They are also induced after infection with different viruses, including papillomavirus and influenza virus.[5,6] IFI44 and IFI44L are composed of 444 and 452 amino acids, respectively, and share 45% amino acid identity.[7] Accumulated evidence suggests a critical role for IFI44 and IFI44L in innate immune responses; however, their biological functions in cancer cells are mostly unknown. A previous study in melanoma cells showed that overexpression of IFI44 leads to suppressed cell proliferation.[8] Similarly, increased IFI44L expression in non-small cell lung carcinoma cells causes reduced proliferation, migration, and invasion.[9] In addition, low IFI44L expression was found in hepatocellular carcinoma (HCC), which shows an antitumor effect through the Met/Src signaling pathway.[10] However, evidence from The Cancer Genome Atlas pan-cancer RNA-sequencing datasets indicates that IFI44 is overexpressed in head and neck squamous cell carcinoma (HNSCC) tumors compared to normal tissues. Furthermore, patients with high IFI44 expression levels are significantly correlated with shorter overall survival (OS) and disease-free survival compared with IFI44-low patients.[11] The functional roles of IFI44 and IFI44L in HNSCC require further investigation.

In the present study, we examined the role of ACSL4 in HNSCC cells and its underlying molecular mechanisms. We showed high expression of ACSL4 in HNSCC tumors and identified the regulatory functions of ACSL4 in HNSCC cell proliferation and invasiveness. Importantly, ACSL4 modulated IFNα/β production and IFN signaling, which promoted IFI44 and IFI44L expression and enhanced cell proliferation and invasiveness. Therefore, ACSL4 could serve as a novel therapeutic target for HNSCC.

2 | MATERIALS AND METHODS

2.1 | Antibodies and chemicals

Antibodies against ACSL1 and ACSL6 were purchased from GeneTex. Antibodies against IFI44 and IFI44L were obtained from ABclonal. The anti-ACSL4 Ab was obtained from Proteintech. The anti-TYK2 Ab was purchased from Cell Signaling Technology. The remaining Abs, including ACSL3, ACSL5, JAK1, signal transducer and activator of transcription 1 (STAT1), interferon regulatory factor 1 (IRF1), and β-actin, were purchased from Santa Cruz Biotechnology. PRGL493 was obtained from MedChemExpress. All other chemicals were obtained from Sigma-Aldrich.

2.2 | Cell culture

Human oral keratinocytes (HOK) were obtained from Applied Biological Materials. HSC-3 cells were purchased from JCRB Cell Bank. FaDu cells were obtained from the Biosource Collection and Research Center (BCRC). 293T, OECM-1, and SAS cells were kindly provided by Dr. Kuo-Wei Chang (National Yang Ming Chiao Tung University). Human oral keratinocytes were cultured in keratinocyte serum-free growth medium (Invitrogen). OECM-1 cells were cultured in RPMI-1640 medium. 293T, FaDu, HSC-3, and SAS cells were cultured in DMEM. Each medium was supplemented with 5% FBS, 2 mM L-glutamine, 100 U/mL penicillin, and 100 μg/mL streptomycin. Cell culture media and supplements were purchased from Invitrogen.

2.3 | Lentiviral production and infection

The lentiviral plasmid carrying Myc-tagged ACSL4 cDNA was purchased from Origene. Lentiviral vectors carrying shRNA targeting the coding sequence of human *ACSL4*, *IFI44*, *IFI44L*, or *IRF1* were obtained from the RNAi Core at Academic Sicina. Lentivirus transfection and production were carried out according to a protocol described previously.[12] For lentiviral infection, cells grown in 60 mm dishes were incubated with viruses in the presence of 8 μg/mL polybrene overnight at 37°C. After refreshing the media, the infected cells were grown for 48 h and then subjected to puromycin selection for 16–24 h.

2.4 | Real-time PCR

Total RNA preparation and real-time PCR protocol were described previously.[13] The paired primers used were: ACSL4 (forward), CATCCCTGGAGCAGATACTCT; ACSL4 (reverse), TCACTTAGGATTTCCCTGGTCC[14]; IRF1 (forward), GCCAGTCGACGAGGATGAGGAAGGGAA; IRF1

(reverse), CCAGCGGCCGCCTGCTACGGTGCACAGG; IFNα (forward), GTACTGCAGAATCTCTCCTTTCTCCTG; IFNα (reverse), GTGTCTAGATCTGACAACCTCCCAGGCACA; IFNβ (forward), TTGTGCTTCTCCACTACAGC; IFNβ (reverse), CTGTAAGTCTGTTAATGAAG[15]; IFI44 (forward), TGGTACATGTGGCTTTGCTC; IFI44 (reverse), CCACCGAGATGTCAGAAAGAG; IFI44L (forward), AAG TGGATGATTGCAGTGAG; IFI44L (reverse), CTCAAT TGCACCAGTTTCCT[7]; GAPDH (forward), GTCTCCT CTGACTTCAACAGCG; and GAPDH (reverse), ACCACCC TGTTGCTGTAGCCAA.[16]

2.5 | Transcriptome sequencing

Total RNA was extracted from cells using TRIzol reagent (Invitrogen). An amount of 1 μg total RNA per sample was used as the input material for RNA sample preparations. Sequencing libraries were generated using the KAPA mRNA HyperPrep Kit (KAPA Biosystems; Roche), following the manufacturer's recommendations, and index codes were added to attribute sequences to each sample. The PCR products were purified using the KAPA Pure Beads system and library quality was assessed using a 100 DNA/RNA Analyzer (BiOptic Inc.). The library was subjected to 150 bp paired-end sequencing and subsequent expression analyses at TOOLS.

2.6 | Detection of IFNα/β concentration

The cells (3×10^5 cells/well) were cultured in 6-well plates. After incubation for 48 h, the cells were treated with PRGL493 or an equal volume of DMSO in 1.5 mL for 16 h. Then supernatants were collected and centrifuged to remove the cells. The concentrations of IFNα and IFNβ in the culture medium were detected using a human IFNalpha ELISA Kit (#BMS216; Invitrogen) and VeriKine Human Interferon Beta ELISA Kit (#41410–1; PBL Assay Science), respectively, according to the manufacturer's instructions.

2.7 | Cell proliferation assay

A density of 5×10^3 cells/well in 100 μL medium was seeded in a 96-well plate. After 24 h of incubation, one set of attached cells in the duplicate wells was added to each well with 10 μL CCK-8 solution (Sigma-Aldrich). After incubating the plate for 2 h, the absorbance was measured at 450 nm using a microplate reader.

2.8 | Migration and invasion assays

An aliquot of 1×10^5 cells was plated on uncoated 24-well inserts with a pore diameter of 8 μm (BD Bioscience) for Transwell migration assays or placed on BioCoat Matrigel invasion chambers (Corning) for invasion assays. Cells were plated in the upper chamber of the Transwell containing 1% FBS-supplemented medium with 2 mM hydroxyurea, which inhibits cell cycle progression, whereas 5% FBS-supplemented medium with 2 mM hydroxyurea was added to the lower chamber. After 24 h, the cells attached to the upper surface of the membrane were wiped off with a cotton bud and the cells on the lower surface were fixed and stained using the Diff-Quik staining kit (BaSO Biotech, Taipei, Taiwan). The migrated or invaded cells were counted from four randomly selected fields in each Transwell membrane under an optical microscope at 100-fold magnification.

2.9 | Cell lysis and immunoblotting

The procedure of cell lysate preparation and western blot analysis were described previously.[12] The relative levels of ACSL4, IFI44, IFI44L, and β-actin protein were semiquantified by densitometric analysis using ImageJ (NIH).

2.10 | Tissue specimens

Paraffin-embedded HNSCC tissue samples, including tumor tissues and noncancerous epithelial tissues at least 2 cm away from the edge of the carcinoma, were obtained from 101 patients with HNSCC from the Department of Pathology and Laboratory Medicine, Kaohsiung Veterans General Hospital between 1996 and 2006. The study protocol was approved by the Institutional Review Board at Kaohsiung Veterans General Hospital (approval code: KSVGH22-CT7-04). None of the patients had received radiation or chemotherapy before surgery.

2.11 | Immunohistochemistry

Formalin-fixed paraffin-embedded tissues were deparaffinized, rehydrated, and subjected to antigen retrieval.[13] The tissue slides were then incubated with anti-ACSL4 Ab (1:300; #22401-1-AP; Proteintech), anti-IFI44 (1:100; #PA5-96967; Thermo Fisher Scientific), or IFI44L (1:20; #PA5-63849; Thermo Fisher Scientific). Subsequently, slides were incubated with secondary Ab and a BOND Polymer Refine Detection System (Leica Biosystems). ACSL4, IFI44, and IFI44L expression were defined by the presence of membranous, and/or cytoplasmic staining, and all tumor cells were evaluated by two independent pathologists. The histological score (HSCORE) was used to evaluate ACSL4, IFI44, and IFI44L immunostaining, which measures the percentage of positively stained cells and the intensity of staining. The intensity score represents the estimated staining intensity of cytoplasmic or membranous immunostaining, scored on a scale of 0 (no staining), 1+ (weak staining), 2+ (moderate staining), and 3+ (strong staining). The percentage (from 0 to 100) of immunostaining cells at each intensity level was multiplied by the

corresponding immunostaining intensity (from 0 to 3) to obtain immunostaining scores ranging from 0 to 300.

2.12 | Statistical analysis

SPSS software version 20.0 (SPSS Inc.), MedCalc for Windows, version 19.1.6 (MedCalc Software), and Prism version 10 (GraphPad Software) were used to undertake statistical analyses. Student's paired *t*-test or one-way ANOVA was applied to determine the significance between groups. Associations between ACSL4 scores and clinicopathologic characteristics were analyzed using the Mann–Whitney *U*-test. The Kaplan–Meier method and log-rank test based on a median cut-off immunoscore value of 90 were used to evaluate significant differences in OS for ACSL4. Associations between categorical variables were evaluated using Fisher's exact test or the χ^2- test. Spearman's correlation coefficient was used to assess the correlation between variables. Statistical significance was set at $p<0.05$.

3 | RESULTS

3.1 | High ACSL4 protein levels were found in HNSCC tissues

Results from the UALCAN database[17] showed that the levels of *ACSL4* gene in primary tumors were significantly higher than those in normal tissues (Figure 1A). The Kaplan–Meier Plotter database[18] further revealed that high *ACSL4* levels (hazard ratio [HR] 1.41, $p=0.034$) were an unfavorable prognostic factor for the OS of patients (Figure 1B). In clinical specimens, ACSL4 proteins showed weak positive staining in the parabasal layer of normal epithelium (Figure 1C,D) and on the cell membrane and cytoplasm of cancerous epithelium with varying staining intensity and distribution (Figure 1E–J). In 75 patients with available normal epithelium and cancerous tissues, ACSL4 showed greater positive expression in tumors than in normal epithelia ($p<0.001$; Figure 1K). Among 101 HNSCC cases, the level of ACSL4 protein was significantly associated with histological stage, pathological grade, tumor extent, lymph node, and distant metastasis. However, no significant difference in gender might be due to the vast difference between male and female sample sizes (Table 1). High ACSL4 protein level was also significantly correlated with a short survival time (Figure 1L; HR 1.891, $p=0.033$).

3.2 | ACSL4 highly expressed in HNSCC cells and regulated cell proliferation and invasiveness

Results from RNA-sequencing analysis of HSC-3 and OECM-1 cells, compared to immortalized HOK, showed the upregulated differentially expressed genes (DEGs) in HSC-3 ($n=511$), OECM-1 ($n=862$), or both cells ($n=471$) (Figure 2A). To explore the potential mechanism of these upregulated DEGs, the Kyoto Encyclopedia of Genes and Genomes (KEGG) enrichment pathway analysis was undertaken. As shown in Figure 2B,C, 10 differential signal pathways were significantly enriched in OECM-1 or HSC-3 cells ($p<0.005$). The DEGs that were upregulated in both cells were mainly associated with pathways related to cell cycle, DNA replication, cellular senescence, and progesterone-mediated oocyte maturation. A heatmap showed the relative expression of these DEGs starting with prefix A and ACSL4 as one of the upregulated genes (Figure 2D). Western blot analysis further indicated that ACSL4, but not the other ACSLs, was highly expressed in all three HNSCC cell lines, which was higher than that in HOK (Figure 2E). Knockdown of ACSL4 expression in OECM-1 cells led to decreased ACSL4 expression, which was approximately 80%–90% lower than that in shCt control cells. However, it did not affect the expression of ACSL1 or ACSL3 (Figure 2F, upper panel). Furthermore, ACSL4-knockdown cells showed a lower proliferation than shCt control cells (Figure 2F, lower panel). Similar results were observed in SAS and HSC-3 cells (Figure 2G,H). ACSL4-knockdown OECM-1 cells also showed reduced migration and invasion, approximately 80% lower than that of shCt control cells (Figure 2I,J). Similar results were found in ACSL4-knockdown HSC-3 cells (Figure 2K,L). The data clearly showed the role of ACSL4 in regulating HNSCC cell proliferation and invasiveness.

3.3 | Silencing ACSL4 expression led to decreased IFI44 and IFI44L expression in HNSCC cells

We further undertook RNA-sequencing analysis to determine differential expression genes between the shCt and ACSL4-knockdown OECM-1 cells. Results from Gene Ontology (GO) analyses revealed that the most enriched biological process terms are associated with the response to the virus and type I IFN signaling pathway (Figure 3A,B). Among 29 downregulated genes with a log2 fold change from −4 to −1 (Figure 3C), we examined whether *IFI44* or *IFI44L*, two IFN-stimulated genes, is the downstream target gene of ACSL4. Data from Figure 3D–F (upper panel) showed that ACSL4-knockdown HNSCC cells showed decreased IFI44 and IFI44L expression. The quantitative results for IFI44 and IFI44L expression in ACSL4-knockdown HNSCC cells are also shown (Figure 3D–F, lower panel). Thus, these results suggest that IFI44 and IFI44L could be downstream effectors of ACSL4 in HNSCC cells.

3.4 | High IFI44 and IFI44L levels in HNSCC tumors correlated with ACSL4 expression

Results from the UALCAN database showed that the expression levels of *IFI44* and *IFI44L* in HNSCC tumors were significantly higher than those in normal tissues ($p<0.001$; Figure 4A,B). Our immunohistochemistry data further revealed that IFI44 and IFI44L proteins were highly expressed in HNSCC tumors compared to

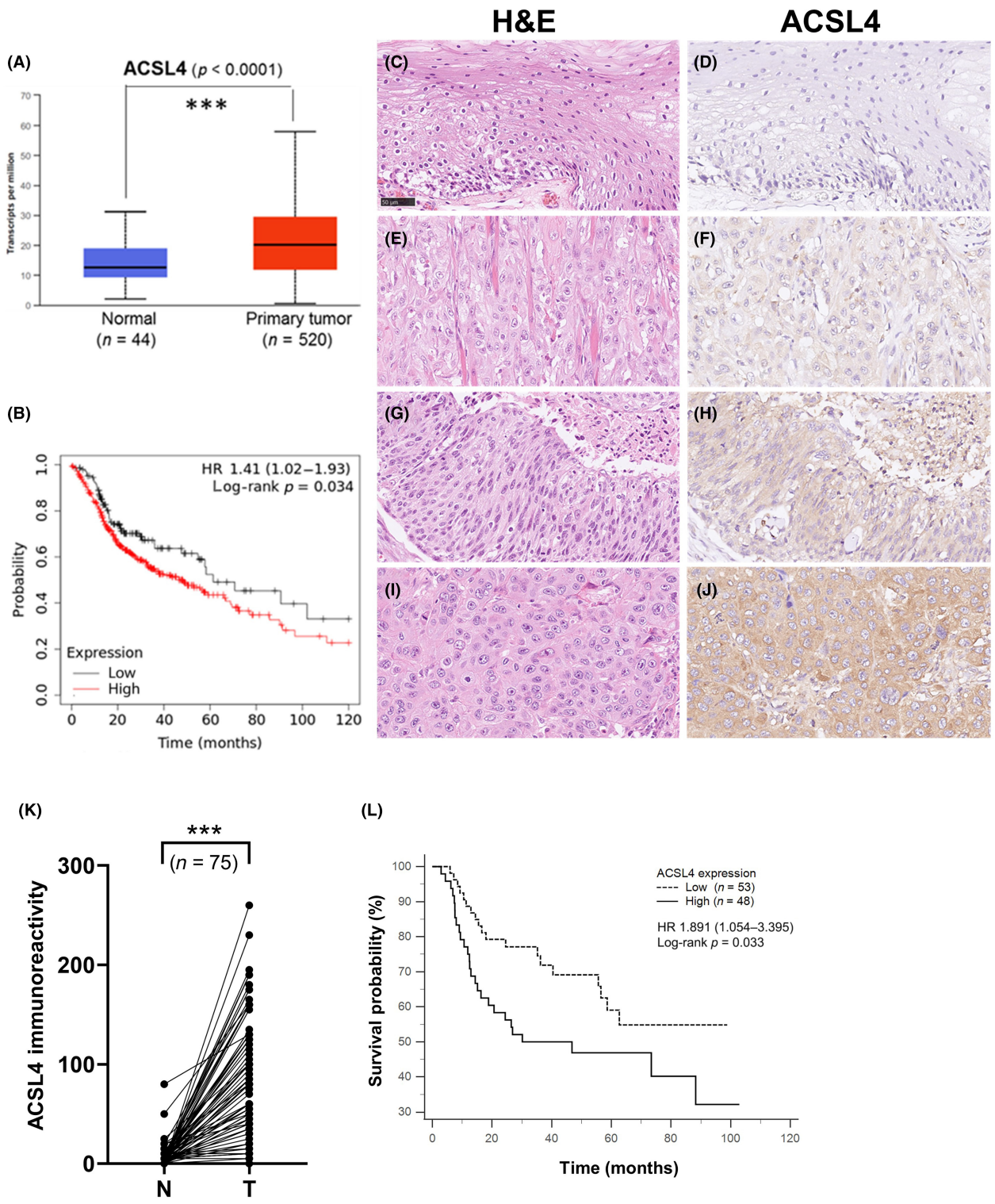

FIGURE 1 Expression of acyl-CoA synthetase 4 (ACSL4) in head and neck squamous cell carcinoma (HNSCC) tissues. (A) Expression of ACSL4 in HNSCC tissues ($n = 520$) and normal head and neck epithelia ($n = 44$). Data were downloaded from the UALCAN database. (B) Kaplan–Meier survival curve shows overall survival for HNSCC patients ($n = 500$) with high (red line) or low (black line) expression of the *ACSL4* gene. The analysis was carried out using the Kaplan–Meier plotter database (http://kmplot.com/analysis/). Using the Kaplan–Meier plots, hazard ratios (HR) with 95% confidence intervals and log-rank *p* values were calculated. (C–J) Representative sections of noncancer epithelia and tumors were stained with H&E and anti-ACSL4 Ab. (C, D) Noncancer epithelia. HNSCC tissues with (E, F) weak (1+), (G, H) moderate (2+), and (I, J) strong (3+) immunoreactivities. Scale bar, 50 μm. (K) Quantification of ACSL4 immunoexpression in 75 paired HNSCC specimens. (L) Kaplan–Meier survival curve in 101 HNSCC patients. High ACSL4 expression was significantly correlated with worse overall survival rates (HR 1.891; $p = 0.033$, log-rank test). ***$p < 0.001$. N, normal epithelium; T, cancerous tissue.

TABLE 1 Relationships between the immunoscore of acyl-CoA synthetase 4 (ACSL4) and clinicopathologic parameters in 101 patients with head and neck squamous cell carcinoma.

		ACSL4 expression		
	Total	Mean ± SEM	Median	*p* value
Age, years[a]				
≤64	89	99.27 ± 6.71	100.0	$p = 0.209$
>64	12	74.17 ± 14.23	80.0	
Gender[a]				
Male	92	97.83 ± 6.34	90.0	$p = 0.275$
Female	9	80.56 ± 25.64	40.0	
Histological grade[b]				
Well	6	46.67 ± 19.22	32.5	$p = 0.007$*
Moderate	85	94.24 ± 6.48	85.0	
Poor	10	143.50 ± 20.35	145.0	
pT stage[a]				
I–II	57	78.86 ± 6.97	75.0	$p = 0.002$*
III–IV	44	118.86 ± 10.05	125.0	
Tumor extent[a]				
T1–2	77	89.81 ± 7.00	80.0	$p = 0.041$*
T3–4	24	117.08 ± 12.44	122.5	
Nodal metastasis[a]				
Positive	34	124.56 ± 12.12	130.0	$p = 0.003$*
Negative	67	81.94 ± 6.38	80.0	
Distant metastasis[a]				
Positive	10	140.00 ± 17.64	132.5	$p = 0.017$*
Negative	91	91.48 ± 6.35	80.0	

[a]*p* value by Mann–Whitney test.

[b]*p* value by Kruskal–Wallis test.

*Significance at $p < 0.05$.

their paired normal epithelia ($p < 0.001$; Figure 4C–E). Furthermore, four HNSCC cell lines showed high IFI44 or IFI44L protein levels, which were higher than those in HOK (Figure 4F). The correlation between ACSL4 levels and IFI44 or IFI44L expression was found in HNSCC tissues. The representative images in Figure 4G show the consistency of ACSL4 with IFI44 or IFI44L immunoreactivity in the same tissues, and the scatter plot in Figure 4H,I indicates a weak to moderate correlation between ACSL4 and IFI44 (rho = 0.375, $p = 0.0001$) or IFI44L (rho = 0.478, $p < 0.0001$) expression. These data collectively suggest that IFIF44 and IFI44L were highly expressed in HNSCC tumors, which was positively correlated with ACSL4 expression.

3.5 | Knockdown of IFI44 or IFI44L led to reduced HNSCC cell proliferation and invasiveness

Next, knockdown of IFI44 expression in HNSCC cells led to decreased IFI44 expression (Figure 5A–C, upper panel). Moreover, IFI44-knockdown cells showed reduced proliferation compared with

FIGURE 2 Expression and functions of acyl-CoA synthetase 4 (ACSL4) in head and neck squamous cell carcinoma (HNSCC) cells. (A) Venn diagram of upregulated genes in HSC-3 cells ($n = 511$), OECM-1 cells ($n = 862$), or both ($n = 471$) compared to HOK. The Kyoto Encyclopedia of Genes and Genomes (KEGG) enrichment pathway analyses for upregulated differentially expressed genes in (B) OECM-1 or (C) HSC-3 cells. (D) Heatmap depicting relative expression of genes starting with the prefix A. Each row indicates a single gene, and each column indicates three sample groups (HOK, HSC-3, and OECM-1). The difference in color in any row showed a differential expression of that particular gene. (E) Total cell lysates were used for immunoblotting with Abs against ACSLs. (F) OECM-1, (G) SAS, and (H) HSC-3 cells were infected with viruses carrying control shRNA (shCt) or ACSL4-targeted shRNAs (shACSL4-1 or shACSL4-3). Total cell lysates were prepared for immunoblotting (upper panel). Proliferation of ACSL4-knockdown HNSCC cells was determined by a CCK-8 assay (lower panel). Data were expressed as the mean ± SD from three independent experiments in triplicate. *$p < 0.05$, **$p < 0.01$, and ***$p < 0.001$ compared with the shCt control cells. Representative images of ACSL4-knockdown (I) OECM-1 or (K) HSC-3 cell migration and invasion. Scale bar, 20 μm. Numbers of migrated or invaded (J) OECM-1 or (L) HSC-3 cells per field are shown as the mean ± SD from two or three independent experiments. Each set of experiments was carried out in duplicate. ***$p < 0.001$ versus the number of shCt control cells. OD, optical density; TNF, tumor necrosis factor.

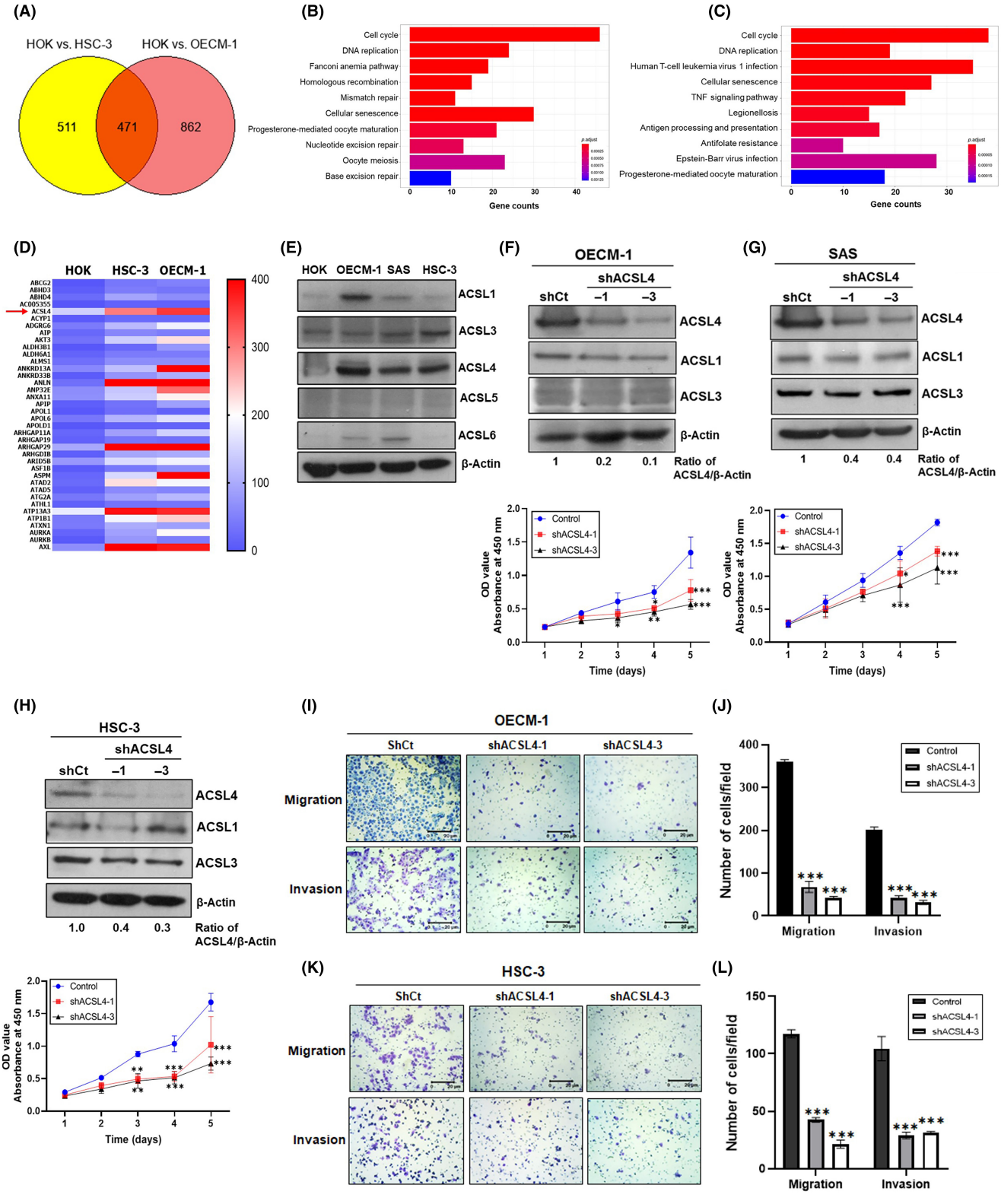

shCt control cells (Figure 5A–C, lower panel). Similar to the results of IFI44 knockdown, the reduction in IFI44L expression in HNSCC cells resulted in decreased cell proliferation (Figure 5D–F). Furthermore, IFI44- and IFI44L-knockdown OECM-1 and HSC-3 cells showed reduced migration and invasion (Figure 5G–J). These data identified the regulatory role of IFI44 and IFI44L in HNSCC cell proliferation and invasiveness.

3.6 | ACSL4 regulated expression of IRF1, JAK1, TYK2, STAT1, IFNα, or IFNβ

Results from Figure 6A showed that overexpression of myc-tagged ACSL4 in OECM-1 cells led to increased protein levels of IRF1, JAK1, tyrosine kinase 2 (TYK2), STAT1, IFI44, and IFI44L. It also increased the expression of *IRF1*, *IFI44*, *IFI44L*, *IFNα*, and *IFNβ* genes (Figure 6B).

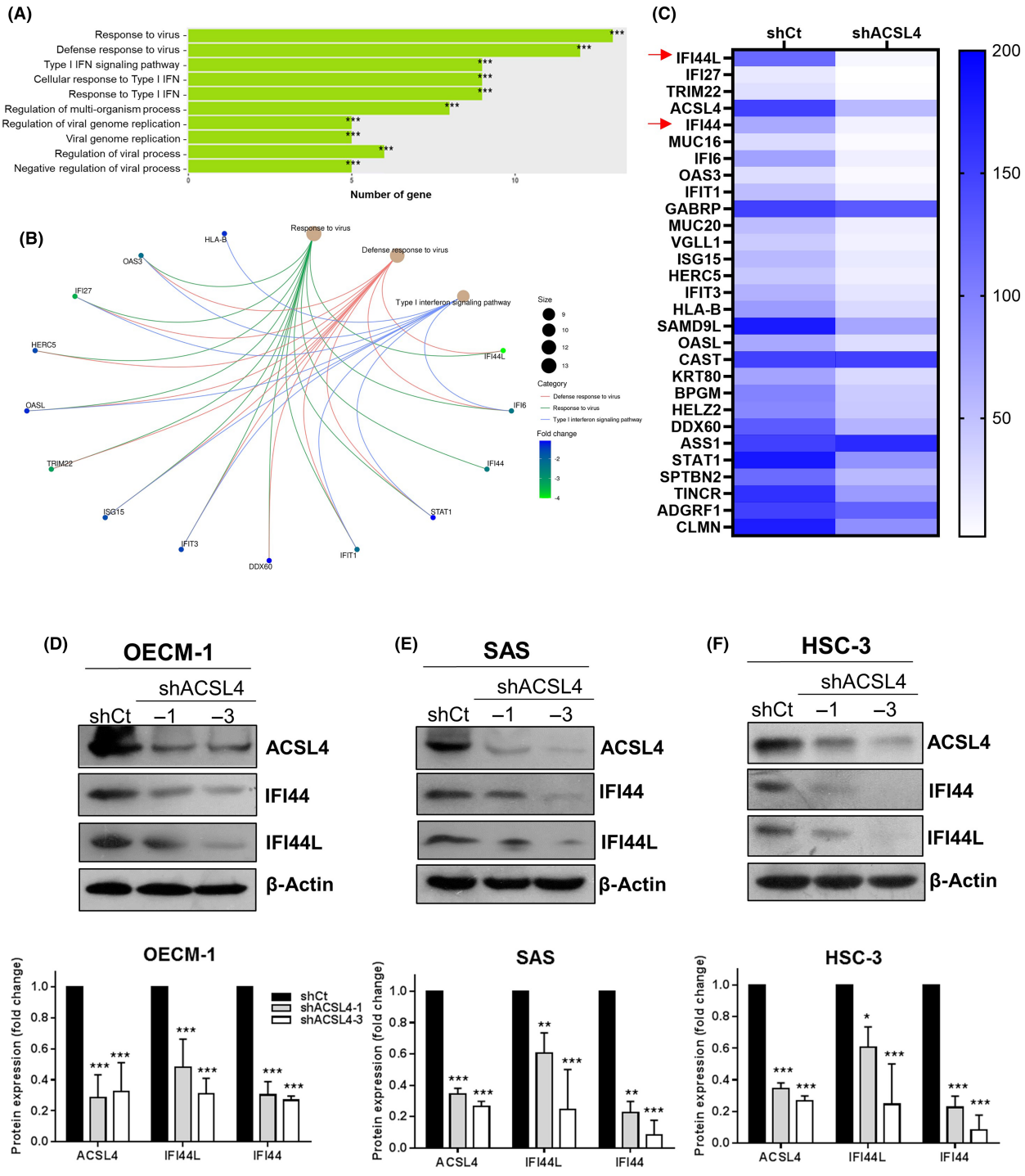

FIGURE 3 Knockdown of acyl-CoA synthetase 4 (ACSL4) in head and neck squamous cell carcinoma cells caused reduced interferon (IFN)-induced protein 44 (IFI44) and IFN-induced protein 44-like (IFI44L) expression. (A) Significantly enriched Gene Ontology (GO) terms of downregulated genes in ACSL4-knockdown OECM-1 cells based on their biological processes (BP). Bar chart shows the top 10 BP terms in the enrichment analysis. (B) Chord plot of Gene Ontology (GO) enrichment analysis. (C) Heatmap indicates the relative expression of downregulated genes between the shCt control and ACSL4-knockdown OECM-1 cells according to the ratio of log2 fold change. (D) OECM-1, (E) SAS, and (F) HSC-3 cells were prepared for western blot analyses. Quantification results of IFI44 and IFI44L expression are shown in the lower panel. Data are expressed as the mean ± SD from two or three independent experiments. $^{*}p < 0.05$, $^{**}p < 0.01$, $^{***}p < 0.001$ versus the ratio of shCt control cells.

In contrast, knockdown of ACSL4 expression in OECM-1 or SAS cells resulted in decreased levels of IRF1, JAK1, TYK2, STAT1, IFI44, and IFI44L proteins (Figure 6C,D). Treatment with PRGL493, a specific ACSL4 inhibitor,[19] in OECM-1 cells suppressed the expression of IRF1, JAK1, TYK2, STAT1, IFI44, and IFI44L in a dose-dependent manner (Figure 6E). The treatment also reduced the mRNA and secreted

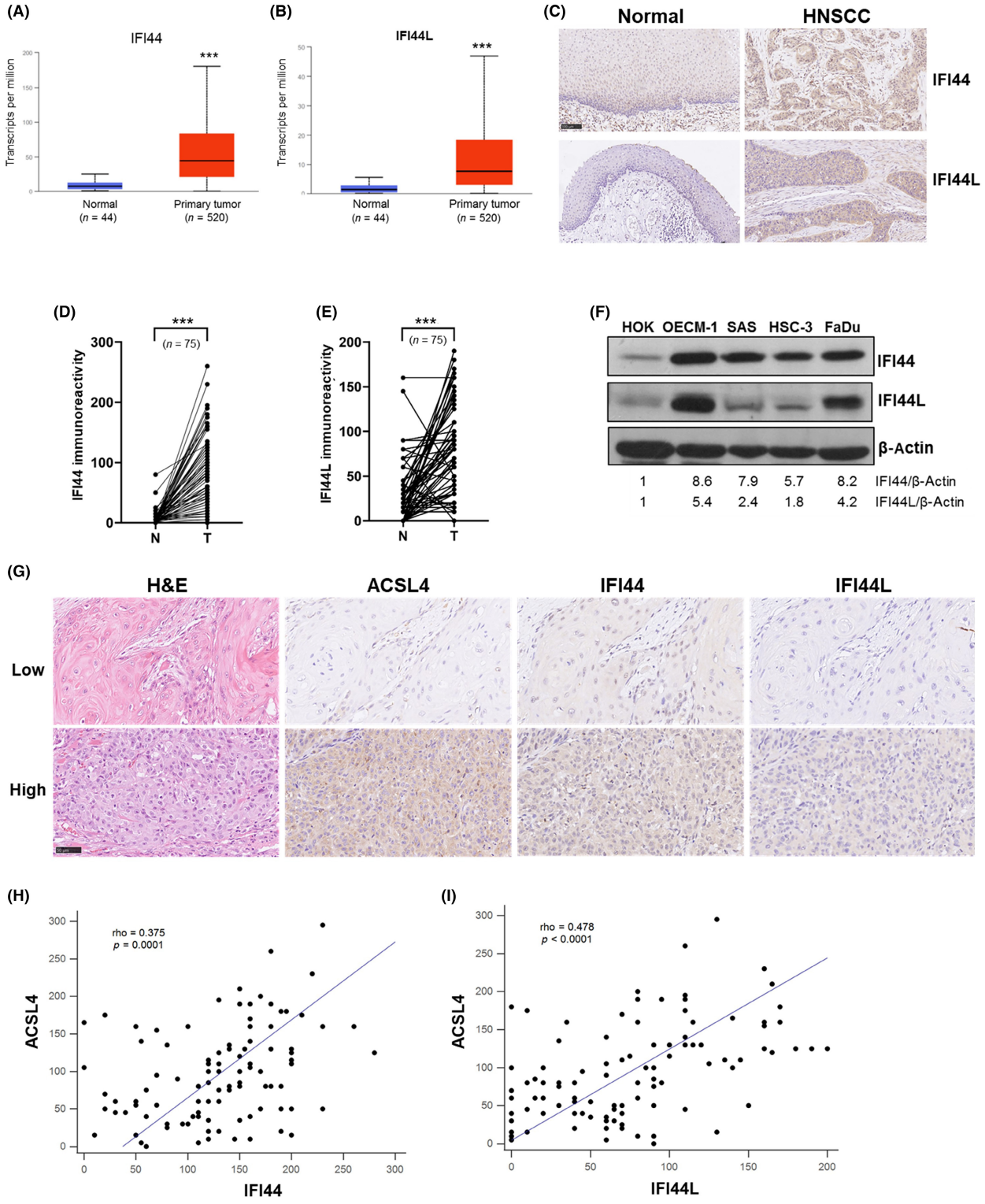

FIGURE 4 Expression of interferon-induced protein 44 (IFI44) or interferon-induced protein 44-like (IFI44L) was correlated with acyl-CoA synthetase 4 (ACSL4) levels in head and neck squamous cell carcinoma (HNSCC) tumors. Results of (A) *IFI44* and (B) *IFI44L* gene expression in HNSCC tumors ($n = 520$) and normal head and neck tissues ($n = 44$) were downloaded from the UALCAN database. (C) Representative normal epithelium and HNSCC tissues were stained with anti-IFI44 or anti-IFI44L antibodies. Quantification of (D) IFI44 or (E) IFI44L immunoexpression in 75 paired HNSCC specimens and significance was determined using the paired t-test. (F) Expression of IFI44 and IFI44L proteins in HOK and HNSCC cells. Protein levels of IFI44 and IFI44L were quantified using ImageJ software and the relative ratio was normalized to the β-actin level. (G) Consistency of ACSL4, IFIF44, and IFI44L immunoreactivity in the same tissue. Representative images of low and high immunostaining for ACSL4, IFI44, and IFI44L are shown. Scale bar, 50 μm. Positive correlation of (H) IFI44 and (I) IFI44L with ACSL4 expression in 101 HNSCC specimens. Spearman's coefficient of rank correlation (rho) and the significance level are shown. ***$p < 0.001$. N, normal epithelium; T, cancerous tissue.

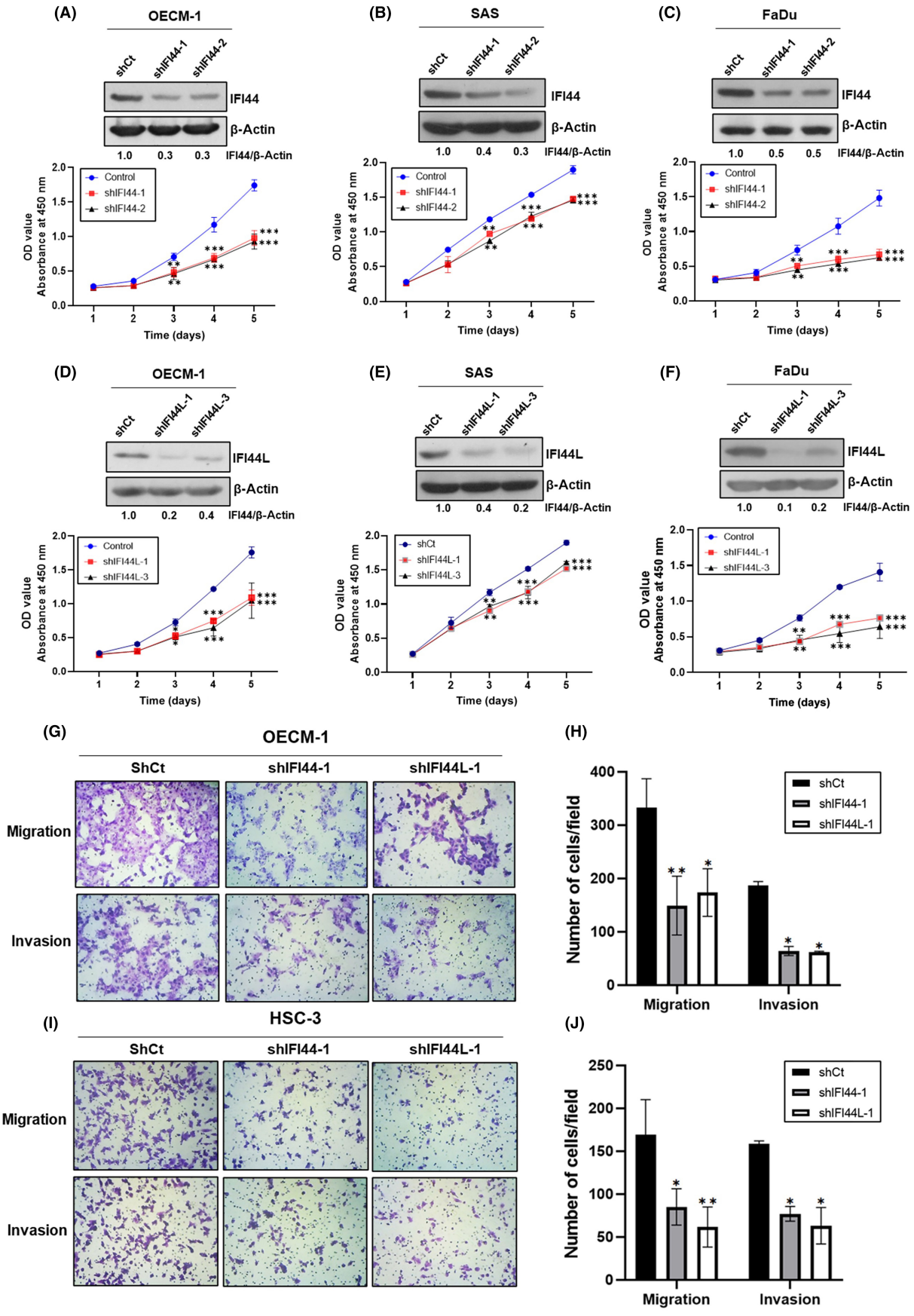
(A)
OECM-1
shCt
shIFI44-1
shIFI44-2
IFI44
β-Actin
1.0 0.3 0.3 IFI44/β-Actin
Control
shIFI44-1
shIFI44-2
OD value Absorbance at 450 nm
Time (days)
(B)
SAS
shCt
shIFI44-1
shIFI44-2
IFI44
β-Actin
1.0 0.4 0.3 IFI44/β-Actin
Control
shIFI44-1
shIFI44-2
OD value Absorbance at 450 nm
Time (days)
(C)
FaDu
shCt
shIFI44-1
shIFI44-2
IFI44
β-Actin
1.0 0.5 0.5 IFI44/β-Actin
Control
shIFI44-1
shIFI44-2
OD value Absorbance at 450 nm
Time (days)
(D)
OECM-1
shCt
shIFI44L-1
shIFI44L-3
IFI44L
β-Actin
1.0 0.2 0.4 IFI44/β-Actin
Control
shIFI44L-1
shIFI44L-3
OD value Absorbance at 450 nm
Time (days)
(E)
SAS
shCt
shIFI44L-1
shIFI44L-3
IFI44L
β-Actin
1.0 0.4 0.2 IFI44/β-Actin
shCt
shIFI44L-1
shIFI44L-3
OD value Absorbance at 450 nm
Time (days)
(F)
FaDu
shCt
shIFI44L-1
shIFI44L-3
IFI44L
β-Actin
1.0 0.1 0.2 IFI44/β-Actin
Control
shIFI44L-1
shIFI44L-3
OD value Absorbance at 450 nm
Time (days)
(G)
OECM-1
ShCt
shIFI44-1
shIFI44L-1
Migration
Invasion
(H)
shCt
shIFI44-1
shIFI44L-1
Number of cells/field
Migration
Invasion
(I)
HSC-3
ShCt
shIFI44-1
shIFI44L-1
Migration
Invasion
(J)
shCt
shIFI44-1
shIFI44L-1
Number of cells/field
Migration
Invasion

FIGURE 5 Effects of knocking down interferon-induced protein 44 (IFI44) or interferon-induced protein 44-like (IFI44L) expression on cell proliferation, migration, and invasion. Total lysates from IFI44-knockdown (A) OECM-1, (B) SAS, or (C) FaDu cells were prepared for immunoblotting. Proliferation of IFI44-knockdown cells was determined by CCK-8 assay. IFI44L-knockdown (D) OECM-1, (E) SAS, or (F) FaDu cells were prepared for western blot analysis or cell proliferation assay. Data were expressed as the mean ± SD from three independent experiments. Each set of experiments was conducted in duplicate. $^{*}p < 0.05$, $^{**}p < 0.01$, versus the ratio of shCt control cells. For the migration and invasion assays, IFI44- or IFI44L-knockdown (G) OECM-1 or (I) HSC-3 cells and the shCt control cells were plated on the Transwell inserts. Representative images are shown at 100-fold magnification. Numbers of migrated or invaded (H) OECM-1 or (J) HSC-3 cells per field are shown as the mean ± SD from two or three independent experiments. Each set of experiments was carried out in duplicate. $^{*}p < 0.05$ and $^{**}p < 0.01$ versus the number of shCt control cells. OD, optical density.

levels of IFNα and IFNβ (Figure 6F–H). Similar results were observed in PRGL493-treated SAS cells (Figure 6I–L). These data suggest that ACSL4 regulated type I IFN signaling and expression, which in turn modulated the expression of IFI44 and IFI44L in HNSCC cells.

3.7 | Knockdown of IRF1 expression suppressed IFN signaling and inhibited cell proliferation and invasiveness

Knockdown of IRF1 in OECM-1 cells caused decreased IFI44 and IFI44L expression. However, it did not affect ACSL4 levels (Figure 7A). Knockdown of IRF1 also suppressed cell proliferation, migration, and invasion (Figure 7B,C) and decreased mRNA levels of *IFNα* and *IFNβ* (Figure 7D). Furthermore, silencing IRF1 expression in SAS and FaDu cells did not affect ACSL4 level, but it led to reduced levels of JAK1, TYK2, IFI44, and IFI44L (Figure 7E,F). These data suggest that IRF1 modulated IFN signaling, cell proliferation, and invasiveness.

4 | DISCUSSION

ACSL4 is an acyl-CoA synthetase involved in arachidonic acid metabolism and ferroptosis induction. However, its function and underlying mechanism in HNSCC cells are yet to be determined. In this study, we demonstrated that ACSL4 was highly expressed in HNSCC tumors and functionally regulated cell proliferation and invasiveness. Importantly, we found that ACSL4 activated type I IFN signaling by upregulating IFNα and IFNβ production, enhancing IFI44 and IFI44L expression and thus promoting HNSCC cell proliferation and invasiveness. The proposed model is shown in Figure 7G. Our study showed the oncogenic functions of ACSL4 in HNSCC cells and its tumor-promoting mechanism. Thus, ACSL4 could serve as a therapeutic target for HNSCC treatment.

Evidence shows that the tumor-suppressive role of ACSL4 in cancer cells is associated with its unique function in promoting ferroptosis. For example, ACSL4 expression is downregulated in lung adenocarcinoma and glioma tissues. Depletion of ACSL4 expression enhances tumor aggressiveness and suppresses ferroptosis.[20,21] However, ACSL4 is highly expressed and performs oncogenic functions in other cancers despite ferroptosis being activated. It has been shown that ACSL4 is highly expressed in multiple myeloma cells, and its expression is essential for enhancing cell proliferation and sensitizing RSL3-induced ferroptosis.[22] A study in the STZ-HFD-treated mouse model also showed that ACSL4-dependent ferroptosis in the liver does not function as an endogenous tumor suppressor but promotes HCC progression following chronic liver damage.[23] Whether ACSL4-dependent ferroptosis acts as a tumor enhancer deserves detailed study; accumulating evidence suggests the oncogenic function of ACSL4.[19,24,25] The oncogenic function of ACSL4 might be mediated by the activation of distinct molecules and signaling pathways in addition to the upregulation of lipid synthesis. For example, ACSL4 upregulates p-AKT, LSD1, and β-catenin in castration-resistant prostate cancer cells.[25] ACSL4 also regulates mTORC1/2 in breast cancer cells and myristoylation of Src kinase in prostate cancer cells.[26,27] Silencing ACSL4 expression abolishes estrogen-induced activation of AKT and GSK3β in breast cancer cells.[28] ACSL4 also causes c-Myc activation, which upregulates the expression of sterol regulatory element-binding protein 1 (SREBP1) and its downstream lipogenic enzymes in HCC cells.[22,29] Our data clearly showed that ACSL4 could upregulate the expression of IFI44 or IFI44L, which promotes the proliferation and invasiveness of HNSCC cells. Limited studies have revealed the tumor suppressive activity of IFI44L in HCC and lung adenocarcinoma.[10,30] However, IFI44L expression is downregulated in those tumor tissues. In contrast, our data showed that IFI44 and IFI44L were highly expressed in HNSCC tumors. Thus, the tumor-promoting or tumor-suppressive function of IFI44 or IFI44L may be closely associated with their expression levels in tumors.

The underlying mechanism by which ACSL4 regulates IFI44 and IFI44L expression is currently unknown. However, our data showed that ACSL4 modulated the expression of IFNα/β, IRF1, TYK2, JAK1, and STAT1, indicating activation of type I IFN signaling. IRF1 is a transcription factor that promotes the expression of IFNα and IFNβ by binding to their promoter regions.[31–33] Thus, ACSL4 could upregulate IRF1 expression and enhance IFNα/β production, which activates IFN signaling and leads to IFI44 and IFI44L expression. Alternatively, elevated expression of IRF1 can directly bind to IFN-stimulated response elements in the promoter region of the *IFI44L* gene, causing gene transcription.[34] A report showed that IFNγ, through IRF1 signaling, stimulates ACSL4 expression and induces cell ferroptosis in mouse melanoma Yumm5.2 cells.[35] However, our data showed that IRF1 did not affect ACSL4 expression in HNSCC cells. Despite different studies reporting the antiproliferative function of IRF1,[36] our data suggested the oncogenic role of IRF1 in

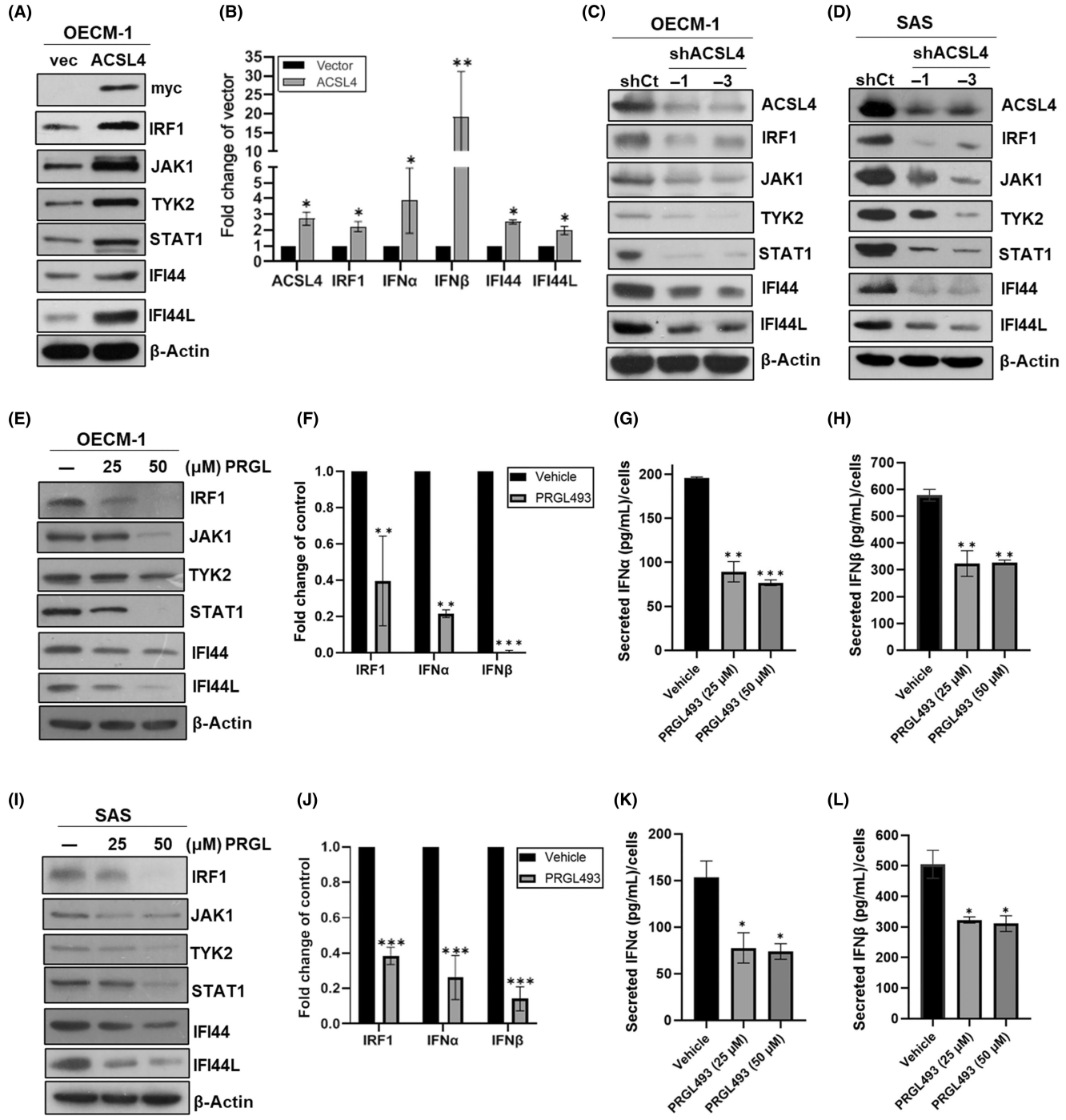

FIGURE 6 Effects of altered acyl-CoA synthetase 4 (ACSL4) expression or activity on interferon (IFN) regulatory factor 1 (IRF1), JAK1, tyrosine kinase 2 (TYK2), signal transducer and activator of transcription 1 (STAT1), IFN-induced protein 44 (IFI44), interferon-induced protein 44-like (IFI44L), IFNα, or IFNβ expression. (A) OECM-1 cells expressing the vector (vec) or myc-tagged ACSL4 were harvested, and total lysates were prepared for western blot analyses. (B) Quantitative PCR analyses of vector control and ACSL4-overexpressed OECM-1 cells. ACSL4-knockdown (C) OECM-1 and (D) SAS cells were prepared for western blot analyses. (E) OECM-1 or (I) SAS cells were treated with 25 μM or 50 μM PRGL493 (PRGL) for 24 h. Cells treated with an equal volume of solvent (DMSO) served as vehicle control. Total lysates were used for western blot analyses. (F) OECM-1 or (J) SAS cells were treated with 25 μM PRGL493 or DMSO for 24 h. Total mRNA was prepared for quantitative PCR analyses. (G, H) OECM-1 or (K, L) SAS cells were treated with PRGL493 or DMSO for 24 h. Cultured media were harvested to analyze the secreted IFNα or IFNβ concentration. Data were expressed as the mean ± SD from two independent experiments in duplicate. $^{*}p < 0.05$, $^{**}p < 0.01$, and $^{***}p < 0.001$ versus the corresponding control cells.

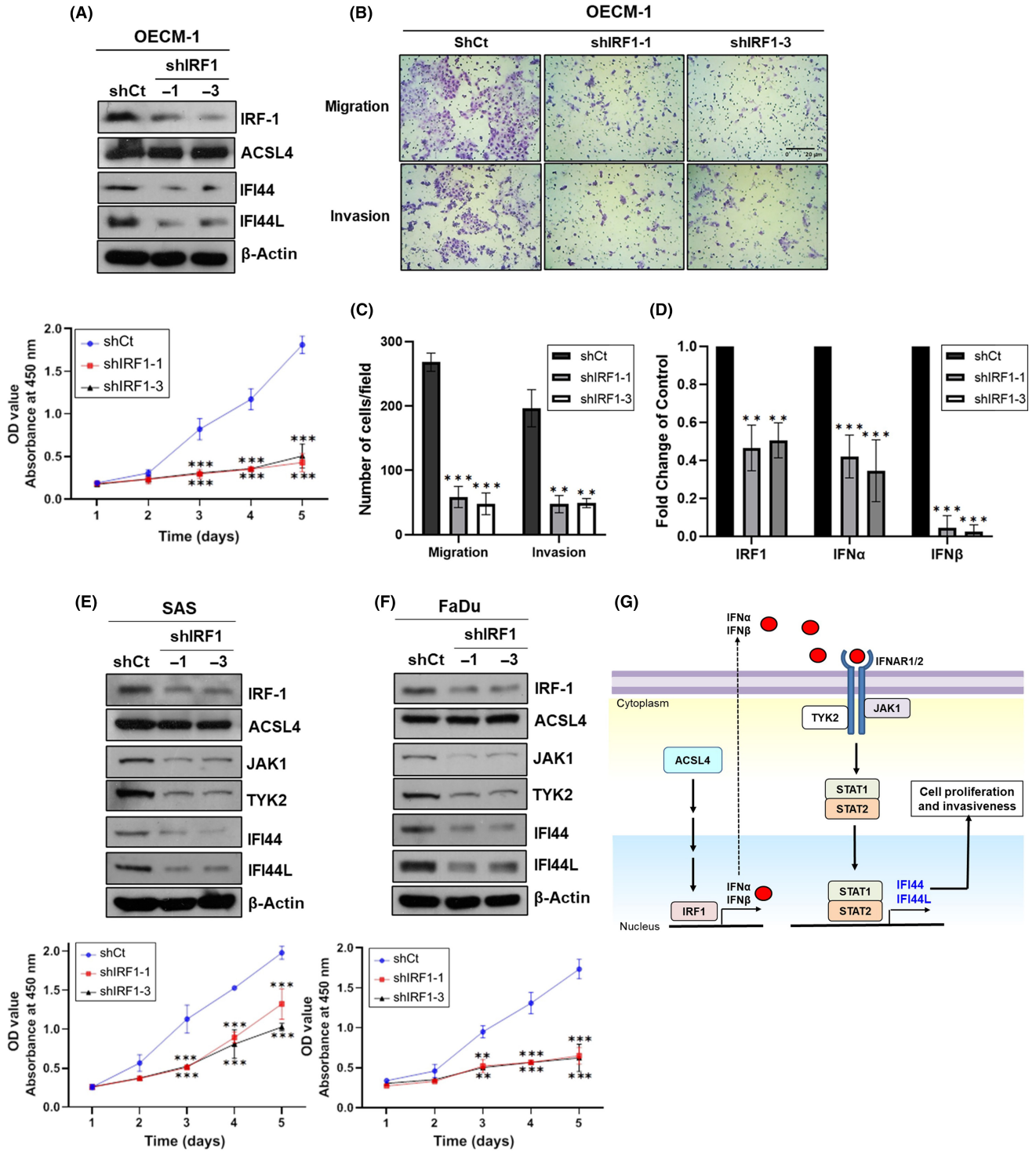

FIGURE 7 Effects of silencing interferon (IFN) regulatory factor 1 (IRF1) expression on acyl-CoA synthetase 4 (ACSL4), JAK1, tyrosine kinase 2 (TYK2), interferon-induced protein 44 (IFI44), and interferon-induced protein 44-like (IFI44L) expression and cell proliferation. (A) IRF1-knockdown OECM-1 cells were prepared for western blot analyses (upper panel) and cell proliferation assays (lower panel). (B) Representative images of migrated or invaded shCt control and shIRF1 OECM-1 cells are shown at 100-fold magnification. Scale bar, 20 μm. (C) Numbers of migrated or invaded cells per field are shown as the mean ± SD from two independent experiments. Each set of experiments was carried out in duplicate. (D) Quantitative PCR analyses of shCt control and IRF1-knockdown OECM-1 cells. (E, F) Western blot analyses and cell proliferation assays of IRF1-knockdown SAS or FaDu cells. $^{**}p < 0.01$ and $^{***}p < 0.001$ versus shCt control cells. (G) Proposed mechanism of how ACSL4 regulated IFI44/IFI44L expression and modulated cell proliferation and invasiveness in head and neck squamous cell carcinoma (HNSCC) cells. Aberrant expression of ACSL4 in HNSCC cells caused increased IRF1 expression, which promoted IFNα/β production and secretion. By binding of IFNα/β receptor (IFNAR1/2), the type I interferon signaling is activated through a TYK2/JAK1/STAT(1/2) pathway. ACSL4 also modulated TYK2, JAK1, and STAT1 expression. It results in increased expression of IFI44 and IFI44L, leading to enhanced cell proliferation and invasiveness. OD, optical density.

HNSCC cells. In addition, results from the UALCAN database revealed high expression levels of *IRF1* in HNSCC tumors.[17] The role of IRF1 in HNSCC malignancy requires further investigation.

Our data clearly showed that ACSL4 could regulate the protein levels of IRF1, JAK1, TYK2, and STAT1. However, the underlying molecular mechanism is unclear. Previous evidence showed that overexpression or depletion of ACSL4 in HCC cells caused altered ERK phosphorylation.[37] Additionally, ACSL4 could promote nuclear factor-κB (NF-κB) signaling in microglia by decreasing the expression of residue-like family member 4 (VGLL4).[38] Interestingly, the human *IRF1* gene contains binding sites for p50 and p65 subunits of NF-κB, indicating that NF-κB could transcriptionally regulate IRF1 expression.[39] As ERK could activate NF-κB activity by phosphorylating IκBα and causing its degradation,[40] ACSL4 may activate ERK/NF-κB signaling to promote IRF1 expression. Although it is unknown how ACSL4 could regulate protein levels of JAK1, TYK2, and STAT1, ACSL4-promoted IRF1 enhances IFNα/β production that activates type I IFN signaling, leading to the phosphorylation of JAK1, TYK2, and STAT1. Phosphorylation of JAK1, TYK2, and STAT1 may also promote their own protein stability. Alternatively, IRF1 restricts hepatitis E virus replication by directly regulating STAT1 expression, resulting in increased levels of total and phosphorylated STAT1 protein.[41]

In summary, our data show that ACSL4 was highly expressed in HNSCC tumors and correlated with poor prognosis in patients. In addition, ACSL4 modulated HNSCC cell proliferation, migration, and invasion. We also identified IFI44 and IFI44L as the downstream effectors of ACSL4. IFI44 and IFI44L were highly expressed in HNSCC tumors and involved in cell proliferation and invasiveness. Importantly, ACSL4 regulated IFNα/β production and IFN signaling, which promoted IFI44 and IFI44L expression. Thus, our data support the oncogenic role of ACSL4 in regulating the proliferation and invasiveness of HNSCC cells by modulating IFN signaling and IFI44/IFI44L expression. Thus, ACSL4 could serve as a potential therapeutic target for treating HNSCC.

AUTHOR CONTRIBUTIONS

Darius Rupa: Formal analysis; investigation; methodology; project administration; software; validation; visualization. **Hao-Wen Chuang:** Formal analysis; investigation; methodology; resources; software; validation; visualization; writing – original draft. **Chung-En Hu:** Formal analysis; investigation. **Wen-Min Su:** Formal analysis; methodology. **Shiou-Rong Wu:** Formal analysis; investigation; methodology. **Herng-Sheng Lee:** Formal analysis; investigation; methodology; visualization. **Ta-Chun Yuan:** Conceptualization; data curation; funding acquisition; project administration; supervision; validation; writing – original draft; writing – review and editing.

ACKNOWLEDGMENTS

We thank Dr. Kuo-Wei Chang at National Yang Ming Chiao Tung University for providing experimental materials. We also thank Taiwan's National Science and Technology Council for the funding support.

FUNDING INFORMATION

This study was supported by grants from the National Science and Technology Council in Taiwan (NSC-111-2314-B-259-001; NSC-112-2314-B-259-001).

CONFLICT OF INTEREST STATEMENT

The authors declare no conflict of interest.

ETHICS STATEMENTS

Approval of the research protocol by an institutional review board: The study protocol was approved by the Institutional Review Board of Kaohsiung Veterans General Hospital (#KSVGH22-CT7-04) in accordance with IRB guidelines and regulations.

Informed consent: The IRB committee approved the waiver of informed consent because all tissue samples were de-identified biospecimens in this study.

Registry and the registration no. of the study/trial: N/A.

Animal studies: N/A.

ORCID

Ta-Chun Yuan https://orcid.org/0000-0001-8359-8383

REFERENCES

1. Hou J, Jiang C, Wen X, et al. ACSL4 as a potential target and biomarker for anticancer: from molecular mechanisms to clinical therapeutics. *Front Pharmacol*. 2022;13:949863.
2. Quan J, Bode AM, Luo X. ACSL family: the regulatory mechanisms and therapeutic implications in cancer. *Eur J Pharmacol*. 2021;909:174397.
3. Kitamura A, Takahashi K, Okajima A, Kitamura N. Induction of the human gene for p44, a hepatitis-C-associated microtubular aggregate protein, by interferon-alpha/beta. *Eur J Biochem*. 1994;224:877-883.
4. Schoggins JW, Wilson SJ, Panis M, et al. A diverse range of gene products are effectors of the type I interferon antiviral response. *Nature*. 2011;472:481-485.
5. Kaczkowski B, Rossing M, Andersen DK, et al. Integrative analyses reveal novel strategies in HPV11,-16 and −45 early infection. *Sci Rep*. 2012;2:515.
6. DeDiego ML, Nogales A, Martinez-Sobrido L, Topham DJ. Interferon-induced protein 44 interacts with cellular FK506-binding protein 5, negatively regulates host antiviral responses, and supports virus replication. *MBio*. 2019;10:10.
7. Busse DC, Habgood-Coote D, Clare S, et al. Interferon-induced protein 44 and interferon-induced protein 44-like restrict replication of respiratory syncytial virus. *J Virol*. 2020;94:e00297-20.
8. Hallen LC, Burki Y, Ebeling M, et al. Antiproliferative activity of the human IFN-alpha-inducible protein IFI44. *J Interf Cytokine Res*. 2007;27:675-680.
9. Zeng Y, Zhang Z, Chen H, et al. Comprehensive analysis of immune implication and prognostic value of IFI44L in non-small cell lung cancer. *Front Oncol*. 2021;11:798425.
10. Huang WC, Tung SL, Chen YL, Chen PM, Chu PY. IFI44L is a novel tumor suppressor in human hepatocellular carcinoma affecting cancer stemness, metastasis, and drug resistance via regulating met/Src signaling pathway. *BMC Cancer*. 2018;18:609.
11. Pan H, Wang X, Huang W, et al. Interferon-induced protein 44 correlated with immune infiltration serves as a potential prognostic indicator in head and neck squamous cell carcinoma. *Front Oncol*. 2020;10:557157.

12. Peng HH, Yang HC, Rupa D, et al. ACK1 upregulated the proliferation of head and neck squamous cell carcinoma cells by promoting p27 phosphorylation and degradation. *J Cell Commun Signal*. 2022;16:567-578.
13. Chuang HW, Pan JH, Cai YX, et al. Reciprocal regulation of CIP2A and AR expression in prostate cancer cells. *Discov Oncol*. 2022;13:87.
14. Spandidos A, Wang X, Wang H, Seed B. PrimerBank: a resource of human and mouse PCR primer pairs for gene expression detection and quantification. *Nucleic Acids Res*. 2010;38:D792-D799.
15. Izaguirre A, Barnes BJ, Amrute S, et al. Comparative analysis of IRF and IFN-alpha expression in human plasmacytoid and monocyte-derived dendritic cells. *J Leukoc Biol*. 2003;74:1125-1138.
16. Nabokina SM, Inoue K, Subramanian VS, Valle JE, Yuasa H, Said HM. Molecular identification and functional characterization of the human colonic thiamine pyrophosphate transporter. *J Biol Chem*. 2014;289:4405-4416.
17. Chandrashekar DS, Bashel B, Balasubramanya SAH, et al. UALCAN: a portal for facilitating tumor subgroup gene expression and survival analyses. *Neoplasia*. 2017;19:649-658.
18. Nagy Á, Munkácsy G, Győrffy B. Pancancer survival analysis of cancer hallmark genes. *Sci Rep*. 2021;11:6047.
19. Castillo AF, Orlando UD, Maloberti PM, et al. New inhibitor targeting acyl-CoA synthetase 4 reduces breast and prostate tumor growth, therapeutic resistance and steroidogenesis. *Cell Mol Life Sci*. 2021;78:2893-2910.
20. Zhang Y, Li S, Li F, Lv C, Yang QK. High-fat diet impairs ferroptosis and promotes cancer invasiveness via downregulating tumor suppressor ACSL4 in lung adenocarcinoma. *Biol Direct*. 2021;16:10.
21. Cheng J, Fan YQ, Liu BH, Zhou H, Wang JM, Chen QX. ACSL4 suppresses glioma cells proliferation via activating ferroptosis. *Oncol Rep*. 2020;43:147-158.
22. Zhang J, Liu Y, Li Q, et al. ACSL4: a double-edged sword target in multiple myeloma, promotes cell proliferation and sensitizes cell to ferroptosis. *Carcinogenesis*. 2023;44:242-251.
23. Grube J, Woitok MM, Mohs A, et al. ACSL4-dependent ferroptosis does not represent a tumor-suppressive mechanism but ACSL4 rather promotes liver cancer progression. *Cell Death Dis*. 2022;13:704.
24. Wu X, Li Y, Wang J, et al. Long chain fatty acyl-CoA synthetase 4 is a biomarker for and mediator of hormone resistance in human breast cancer. *PLoS One*. 2013;8:e77060.
25. Wu X, Deng F, Li Y, et al. ACSL4 promotes prostate cancer growth, invasion and hormonal resistance. *Oncotarget*. 2015;6:44849-44863.
26. Orlando UD, Castillo AF, Dattilo MA, Solano AR, Maloberti PM, Podesta EJ. Acyl-CoA synthetase-4, a new regulator of mTOR and a potential therapeutic target for enhanced estrogen receptor function in receptor-positive and -negative breast cancer. *Oncotarget*. 2015;6:42632-42650.
27. Ma Y, Zhang X, Alsaidan OA, et al. Long-chain acyl-CoA synthetase 4-mediated fatty acid metabolism sustains androgen receptor pathway-independent prostate cancer. *Mol Cancer Res*. 2021;19:124-135.
28. Belkaid A, Ouellette RJ, Surette ME. 17β-estradiol-induced ACSL4 protein expression promotes an invasive phenotype in estrogen receptor positive mammary carcinoma cells. *Carcinogenesis*. 2017;38:402-410.
29. Chen J, Ding C, Chen Y, et al. ACSL4 reprograms fatty acid metabolism in hepatocellular carcinoma via c-Myc/SREBP1 pathway. *Cancer Lett*. 2021;502:154-165.
30. Zeng Y, Chen HQ, Zhang Z, et al. IFI44L as a novel epigenetic silencing tumor suppressor promotes apoptosis through JAK/STAT1 pathway during lung carcinogenesis. *Environ Pollut*. 2023;319:120943.
31. Harada H, Willison K, Sakakibara J, Miyamoto M, Fujita T, Taniguchi T. Absence of the type I IFN system in EC cells: transcriptional activator (IRF-1) and repressor (IRF-2) genes are developmentally regulated. *Cell*. 1990;63:303-312.
32. Escalante CR, Yie J, Thanos D, Aggarwal AK. Structure of IRF-1 with bound DNA reveals determinants of interferon regulation. *Nature*. 1998;391:103-106.
33. Tamura T, Yanai H, Savitsky D, Taniguchi T. The IRF family transcription factors in immunity and oncogenesis. *Annu Rev Immunol*. 2008;26:535-584.
34. Li Y, Zhang J, Wang C, Qiao W, Li Y, Tan J. IFI44L expression is regulated by IRF-1 and HIV-1. *FEBS Open Bio*. 2021;11:105-113.
35. Liao P, Wang W, Wang W, et al. CD8(+) T cells and fatty acids orchestrate tumor ferroptosis and immunity via ACSL4. *Cancer Cell*. 2022;40:365-378.e6.
36. Alsamman K, El-Masry OS. Interferon regulatory factor 1 inactivation in human cancer. *Biosci Rep*. 2018;38:BSR20171672.
37. Chen J, Ding C, Chen Y, et al. ACSL4 promotes hepatocellular carcinoma progression via c-Myc stability mediated by ERK/FBW7/c-Myc axis. *Oncogenesis*. 2020;9:42.
38. Zhou X, Zhao R, Lv M, et al. ACSL4 promotes microglia-mediated neuroinflammation by regulating lipid metabolism and VGLL4 expression. *Brain Behav Immun*. 2023;109:331-343.
39. Iwanaszko M, Kimmel M. NF-kappaB and IRF pathways: cross-regulation on target genes promoter level. *BMC Genomics*. 2015;16:307.
40. Chen B, Liu J, Ho TT, Ding X, Mo YY. ERK-mediated NF-kappaB activation through ASIC1 in response to acidosis. *Oncogenesis*. 2016;5:e279.
41. Perevalova AM, Gulyaeva LF, Pustylnyak VO. Roles of interferon regulatory factor 1 in tumor progression and regression: two sides of a coin. *Int J Mol Sci*. 2024;25:2153.

How to cite this article: Rupa D, Chuang H-W, Hu C-E, et al. ACSL4 upregulates IFI44 and IFI44L expression and promotes the proliferation and invasiveness of head and neck squamous cell carcinoma cells. *Cancer Sci*. 2024;115:3026-3040. doi:10.1111/cas.16236